






# Combating Intracellular Pathogens with Nano-hybrid-Facilitated Antibiotic Delivery

This article was published in the following Dove Press journal:  
*International Journal of Nanomedicine*

Rajendran JC Bose <sup>1-4,\*</sup>  
Nagendran Tharmalingam <sup>5,\*</sup>  
Yonghyun Choi<sup>1</sup>  
Thiagarajan Madheswaran <sup>6</sup>  
Ramasamy Paulmurugan <sup>2,3</sup>  
Jason R McCarthy <sup>4</sup>  
Soo-Hong Lee<sup>7</sup>  
Hansoo Park<sup>1</sup>

<sup>1</sup>School of Integrative Engineering, Chung-Ang University, Seoul, South Korea; <sup>2</sup>Molecular Imaging Program at Stanford (MIPS), Department of Radiology, School of Medicine, Stanford University, Stanford, CA 94305-5427, USA; <sup>3</sup>Canary Center at Stanford for Cancer Early Detection, Department of Radiology, School of Medicine, Stanford University, Stanford, CA 94305-5427, USA; <sup>4</sup>Masonic Medical Research Institute, Utica, NY, USA; <sup>5</sup>Infectious Diseases Division, Warren Alpert Medical School of Brown University, Rhode Island Hospital, Providence, RI 02903, USA; <sup>6</sup>Department of Pharmaceutical Technology, School of Pharmacy, International Medical University, Kuala Lumpur 57000, Malaysia; <sup>7</sup>Department of Medical Biotechnology, Dongguk University, Seoul, Gyeonggi-do, South Korea

\*These authors contributed equally to this work

Correspondence: Soo-Hong Lee  
Department of Medical Biotechnology,  
Dongguk University, Seoul, Gyeonggi-do,  
South Korea  
Tel +82-31-961-5153  
Email soohong@dongguk.edu

Hansoo Park  
School of Integrative Engineering, Chung-  
Ang University, Seoul, South Korea  
Tel +82 2-820-5804  
Email heyshoo@cau.ac.kr

**Background:** Lipid polymer hybrid nanoparticles (LPHNPs) have been widely investigated in drug and gene delivery as well as in medical imaging. A knowledge of lipid-based surface engineering and its effects on how the physicochemical properties of LPHNPs affect the cell–nanoparticle interactions, and consequently how it influences the cytological response, is in high demand.

**Methods:** Herein, we have engineered antibiotic-loaded (doxycycline or vancomycin) LPHNPs with cationic and zwitterionic lipids and examined the effects on their physicochemical characteristics (size and charge), antibiotic entrapment efficiency, and the in vitro intracellular bacterial killing efficiency against *Mycobacterium smegmatis* or *Staphylococcus aureus* infected macrophages.

**Results:** The incorporation of cationic or zwitterionic lipids in the LPHNP formulation resulted in a size reduction in LPHNPs formulations and shifted the surface charge of bare NPs towards positive or neutral values. Also observed were influences on the drug incorporation efficiency and modulation of the drug release from the biodegradable polymeric core. The therapeutic efficacy of LPHNPs loaded with vancomycin was improved as its minimum inhibitory concentration (MIC) (2 µg/mL) versus free vancomycin (4 µg/mL). Importantly, our results show a direct relationship between the cationic surface nature of LPHNPs and its intracellular bacterial killing efficiency as the cationic doxycycline or vancomycin loaded LPHNPs reduced 4 or 3 log CFU respectively versus the untreated controls.

**Conclusion:** In our study, modulation of surface charge in the nanomaterial formulation increased macrophage uptake and intracellular bacterial killing efficiency of LPHNPs loaded with antibiotics, suggesting alternate way for optimizing their use in biomedical applications.

**Keywords:** nano-hybrids, intracellular bacterial infection, *Mycobacterium smegmatis*, *Staphylococcus aureus*, doxycycline, vancomycin

## Introduction

The treatment of intracellular bacterial infections is often challenging for clinicians, and novel therapies are needed.<sup>1</sup> Intracellular infections can be recurrent and difficult to treat, owing to the low availability of antibiotics in infected cells and insufficient host defenses.<sup>2</sup> *Mycobacterium tuberculosis*, *Salmonella typhimurium*, and *Staphylococcus aureus*<sup>3</sup> are the main intracellular bacteria found inside the macrophages, where they act like a “Trojan horse” to cause recurrent infections at secondary sites.<sup>2</sup> Intracellular bacterial infections typically require long-term antibiotic intake, which may lead to poor compliance and contribute to developing resistant strain.<sup>4</sup> Besides, most conventional antibiotics exhibit poor intracellular penetration and retention ability, which

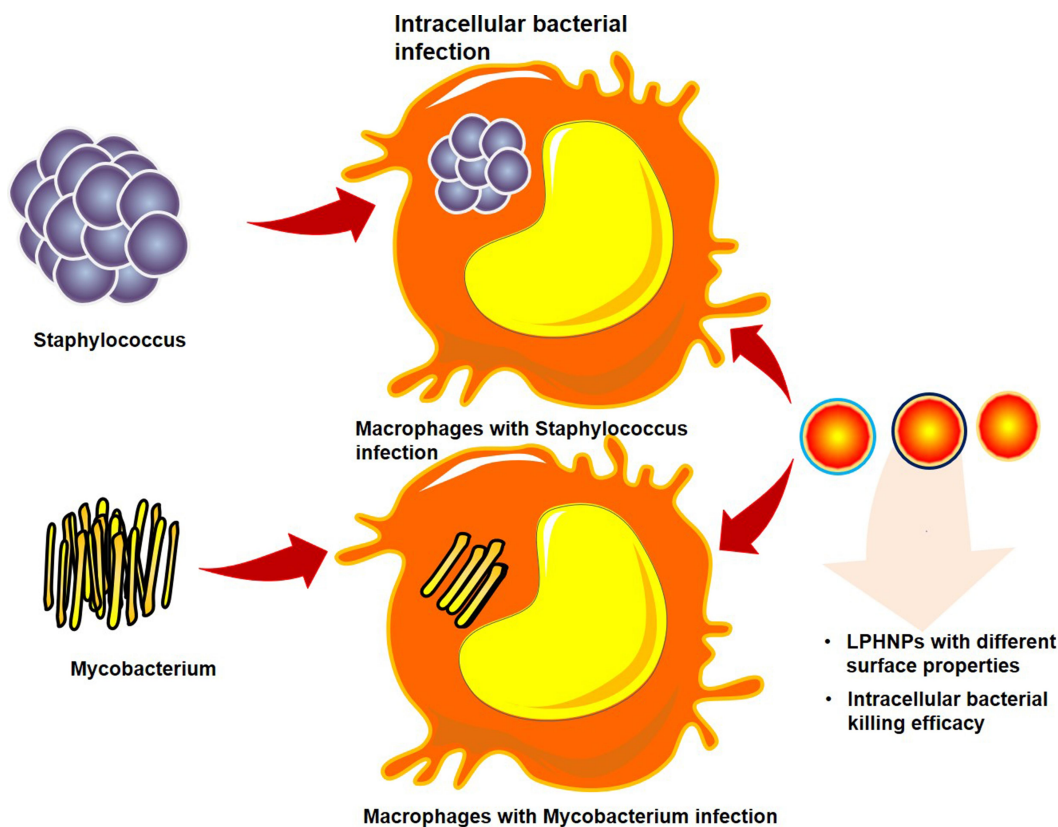


**Figure 1** The schematic diagram outlines the overall concept of the experiment. The cationic and zwitterionic lipids-based surface engineering approach with antibiotics (doxycycline or vancomycin) loaded LPHNPs were prepared and examined their surface charge influence on the physicochemical characteristics, antibiotic entrapment, and intracellular release behaviors against *Mycobacterium smegmatis* or *Staphylococcus aureus* infected macrophages in vitro.

leads to a relapse of infection and antibiotic resistance.<sup>5</sup> Engineered nanoparticles (NPs) are helping to counteract the intracellular antibiotic delivery.<sup>6–10</sup> The intracellular delivery of antibiotics associated with engineered NPs offers significant advantages over free drugs, including an improved drug efficacy by protection from degradation, optimal therapeutic levels at the site of bacterial infection via sustained release, and a reduced dosing frequency, thereby minimizing drug-associated toxicity.<sup>11</sup> Several engineered NPs, liposomes, and cell-derived vesicles have been evaluated for antibiotic delivery.<sup>12,13</sup> However, a low encapsulation efficiency, high burst release, cytotoxicity, and poor stability have limited their clinical success.<sup>2</sup> Lipid-polymer hybrid nanoparticles (LPHNPs) can overcome the issues associated with polymeric NPs and liposomes.<sup>14–17</sup> LPHNPs are core-shell hybrid nanostructures, theoretically derived from both liposome and polymeric nanomaterials, where polymeric nanomaterials are enveloped by a lipid layer. Compared with conventional nanocarriers, LPHNPs exhibit enhanced cell interactions, higher drug loading, and controlled drug release.<sup>16,18–20</sup> We previously reported that

the coating of lipids of different types on the PLGA-NP core influences the size, surface charge, therapeutic loading efficiency, including gene and small molecules, and controlled release ability.<sup>15,18,19</sup> Furthermore, the nature and charge of the NPs surface are crucial determinants of the macrophage recognition and phagocytosis mechanism.<sup>20</sup> Therefore, in the present study, we developed a cationic and zwitterionic lipids-based surface engineering approach with antibiotics (Doxycycline or Vancomycin) loaded LPHNPs and examined the intracellular antibacterial activity of drug-loaded LPHNPs against in vitro model of *Mycobacterium smegmatis* (*M. smegmatis*) or *Staphylococcus aureus* (*S. aureus*) infected macrophages to determine the optimal formulation.

## Materials and Methods

### Bacterial Strain and Macrophages

The bacteria and macrophages were obtained from our laboratory resources. The bacterial cultures were methicillin-resistant *Staphylococcus aureus* (MRSA) (ATCC BAA 1683) and *Mycobacterium smegmatis* (ATCC 607).<sup>5,35</sup> The mouse leukemic monocyte-macrophage

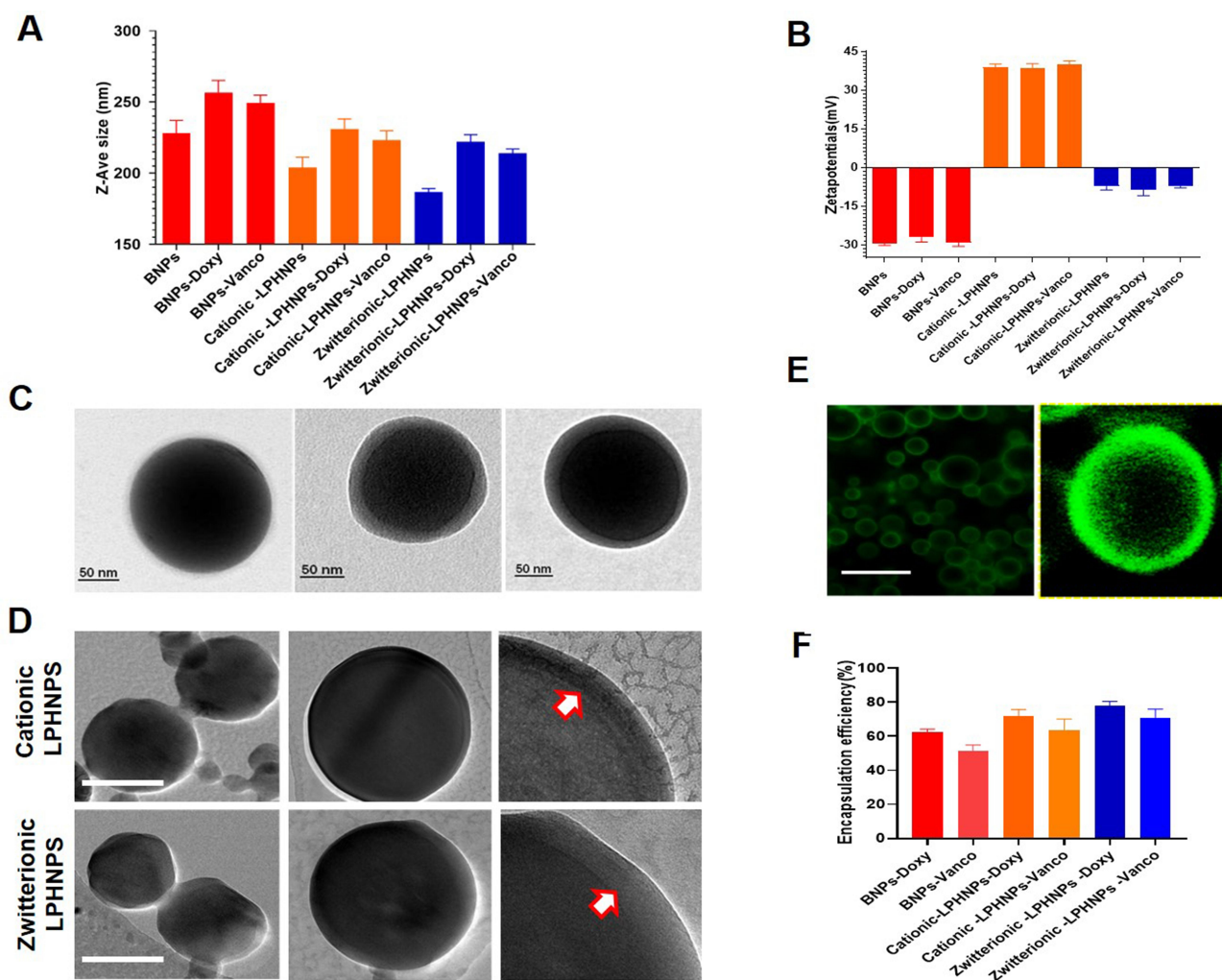


**Figure 2** Physicochemical characterization of cationic or zwitterionic lipid polymer hybrid and non-lipid layered nanoparticles loaded with either doxycycline or Vancomycin. **(A)** DLS based Size analysis of different Nanoparticles formulations. **(B)** Surface-charge ( $\zeta$ -potentials) analysis of different nanoparticle formulations measured by Malvern Zeta sizer. **(C)** EFTEM images of non-lipid layered, zwitterionic, and cationic lipid polymer hybrid nanoparticles. **(D)** Cryo-electron microscopy analysis of cationic or zwitterionic lipid polymer hybrid nanoparticles, Arrow marks indicate the lamellar assembly lipids on Polymer-NPs (Scale bar:0.2 $\mu$ m). **(E)** CLSM image of fluorescent lipid layered LPHNPs. **(F)** The encapsulation efficiency of cationic or zwitterionic lipid polymer hybrid and non-lipid layered nanoparticles loaded with either doxycycline or vancomycin.

cells RAW 264.7 (ATCCTIB-71) and macrophage cells J774A.1 (ATCC TIB-67) were used for all cell culture experiments.<sup>2,36</sup>

## Chemicals

The antibiotics (Vancomycin and doxycycline), PLGA (50:50), and polyvinyl alcohol (PVA; molecular weight 13–23 kDa) were purchased from Sigma-Aldrich (St. Louis, MO, USA). The lipids 1,2-dioleoyl-3-trimethylammonium-propane (chloride salt) (DOTAP), 1, 2-distearoyl-sn-glycero-3-phosphoethanolamine *N*-[methoxy-(polyethylene glycol)-2000] (ammonium salt) (DSPE-PEG), 1, 2-dioleoyl-sn-glycerol-3-phosphocholine (DOPC), and fluorescent lipid 1-oleoyl-2-[12-[(7-nitro-2-1,3-benzoxadiazol-4-yl)amino]

dodecanoyl]-sn-glycero-3-phosphocholine] (NBD-PC) were purchased from Avanti Polar Lipids (Alabaster, AL, USA). The dye 1, 10-dioctadecyl-3, 3', 3'', 3'''-tetramethylindodicarbocyanine, 4-chlorobenzenesulfonate salt (DiD) was purchased from Invitrogen (Eugene, OR, USA). Nutrient Broth, Mueller-Hinton Broth (MHB), and Mueller-Hinton Agar (MHA) were obtained from Biolab (Midrand, South Africa). Middlebrook 7H9 broth medium (Becton Dickinson GmbH, Heidelberg, Germany). The LIVE/DEAD BacLight Bacterial Viability Kit was purchased from Molecular Probes (Eugene, OR, USA). All other chemicals and reagents were purchased from Sigma-Aldrich Co. unless otherwise stated.

## Preparation of Antibiotic-Loaded LPHNPs and BNPs

The antibiotic (doxycycline or vancomycin)-loaded LPHNPs were prepared as described previously, with slight changes in the modified emulsion solvent-evaporation method.<sup>15,19</sup> Briefly, the antibiotic (doxycycline or vancomycin (0.5:1) was dissolved in an aqueous buffer solution. The cationic lipid DOTAP or DOPC (15% w/w to the polymer) and PLGA (3%) were dissolved in dichloromethane. The w/o emulsion was prepared by the addition of antibiotic-containing aqueous buffer to the PLGA solution with sonication (Ultrasonic Probe; Sonics & Materials Inc., Newtown, CT, USA). The resulting w/o emulsion was transferred into a stabilizer (1% w/v PVA) solution and sonicated in an ice bath. The resultant w/o/w emulsion was stirred until the evaporation process was complete. Finally, the antibiotic encapsulated LPHNPs were separated by ultracentrifugation and freeze-dried. Blank, fluorescent (DiD or NBD-PC lipid) nanoparticles were also prepared using the same conditions, with few modifications.<sup>18,19</sup>

## Characterization of LPHNPs and BNPs

The particle size (*z*-average) and size distribution (polydispersity index) of blank, antibiotic-loaded BNPs and LPHNPs were measured by dynamic light scattering (DLS) using a Zetasizer Nano ZS (Malvern Instruments), and the surface charges (Zeta potential) of all formulations were determined as described previously. The morphological analysis of all formulations was investigated by field-emission scanning electron microscopy (FESEM; JSM-6700F; JEOL, Tokyo, Japan) at an accelerating voltage of 5 kV.<sup>19,39</sup> The hybrid nature of LPHNPs was visualized by energy-filtered transmission electron microscopy (EFTEM). EFTEM experiments were performed using a Libra 120 microscope (Carl Zeiss Meditec AG, Jena, Germany), and samples were prepared by depositing 20  $\mu$ L of the LPHNPs suspension (0.5 mg/mL) onto a 200-mesh carbon-coated copper grid.<sup>15,19</sup> The lipid layers on PLGA NPs were analyzed by Cryo-TEM using a Tecnai G2 20 TWIN transmission electron microscope (FEI, Hillsboro, OR, USA). Samples for Cryo-TEM were prepared using an FEI Vitrobot Mark IV, under controlled temperature and humidity conditions within an environmental vitrification system. A small droplet (5  $\mu$ L) was deposited onto a Pelco Lacey carbon-film grid and spread carefully. Excess liquid was removed, resulting in the formation of a thin (10–500 nm) sample film.<sup>27,40</sup>

Additionally, the presence of the assembled lipid layer on the PLGA NP core was further confirmed by confocal laser scanning microscopy (CLSM; Carl Zeiss LSM 510 Meta) with fluorescent NBD-PC.<sup>18,19,28</sup>

## Antibiotic(s) Encapsulation Efficiency and Release Behavior

The loading efficiency of doxycycline or vancomycin in BNPs or LPHNPs was quantified by spectrophotometry (UV-160; Shimadzu, Tokyo, Japan) by measuring the amount of non-entrapped doxycycline or vancomycin in the external aqueous solution.<sup>41,42</sup> The external aqueous solution was obtained after centrifugation of the colloidal suspension for 30 min at  $18,000 \times g$ . In vitro drug release was performed for 120 h at 37°C. Antibiotic-encapsulated BNPs and LPHNPs were suspended in 3 mL of PBS with continuous shaking. The eluted doxycycline or vancomycin was withdrawn at predetermined time points, and an equal volume of fresh buffer was replaced at every sampling point. The samples were analyzed by UV spectrophotometry, as described above.

## Determination of Minimum Inhibitory Concentrations

The minimum inhibitory concentrations (MICs) of drug-free and Doxy- or Vanco-loaded BNP and LPHNP formulations were determined against *M. smegmatis* or *S. aureus*.<sup>5,35</sup> Cultures were grown in 10 mL of broth (Middlebrook or MHB) overnight at 37°C with shaking at 200 rpm. These cultures were then washed and diluted to a final concentration of  $5 \times 10^5$  bacteria/mL, and various concentrations of doxycycline or vancomycin-encapsulated NPs or standard concentrations of free antibiotics were added separately. After 18 h of incubation at 37°C and shaking at 200 rpm, bacterial densities were estimated by diluting and plating on agar followed by incubation overnight at 37°C.

## Cytotoxicity Assay

The cytotoxicity of BNPs and LPHNPs on macrophages was evaluated by CCK-8 assays.<sup>18,19</sup> J774.1 ( $5 \times 10^3$ ) cells were seeded in 96-well plates and incubated in DMEM containing 10% FBS 24 h before the experiment. Serially diluted BNPs and LPHNPs in serum-free DMEM were added to the cells and incubated for 24 h at 37°C.<sup>43,44</sup> CCK-8 solution (10  $\mu$ L) was added to each well, followed by incubation for 1 h at 37°C. Then, absorbance at 450 nm was measured using a microplate reader (BioTek Instruments, Inc., Winooski, VT, USA).

**Table I** Minimum Inhibitory Concentration Assay of Non-Lipid Layered BNPs and Cationic or Zwitterionic LPHNPs Loaded with Doxycycline or Vancomycin with Controls

Compounds	MIC ( $\mu\text{g}\cdot\text{mL}^{-1}$ )
Doxycycline	4
Bare PLGA NPs with doxycycline (F1B)	16
Cationic LPHNPs with doxycycline (F2B)	4
Zwitterionic LPHNPs with doxycycline (F3B)	16
Vancomycin	4
Bare PLGA NPs with vancomycin (F1C)	16
Cationic LPHNPs with vancomycin (F2C)	2
Zwitterionic LPHNPs with vancomycin (F3C)	32

## Intracellular Uptake of BNPs and LPHNPs by Macrophages

The J774.1 ( $1.8 \times 10^5$ ) cells were seeded before 18 h of treatment. The cells were then incubated with fluorescent BNPs and LPHNPs for 24 h at  $37^\circ\text{C}$ . After incubation cells were washed and treated with 0.25% trypsin for 10 min, and cells were resuspended directly in PBS for cytometry (FACS). Cell suspensions were analyzed by flow cytometry (Accuri C6; BD Biosciences, Franklin Lakes, NJ, USA).<sup>18–20,26</sup> All measurements were performed in triplicate or more. Particle uptake by macrophages was further visualized by CLSM.<sup>2,18,19,33</sup> Briefly, J774.1 cell ( $8 \times 10^4$ ) was cultured on a coverslip and incubated at  $37^\circ\text{C}$  in a 5%  $\text{CO}_2$  incubator for 24 h. Then, fluorescent NPs (BNPs and cationic and zwitterionic LPHNPs) were added to the J774.1 cell and incubated for an additional 24 h. Then, these cells were washed twice with PBS and fixed with a paraformaldehyde solution. The fixed J774.1 cell was stained with DAPI and visualized by CLSM (TCS SP5 II; Leica, Heidelberg, Germany).

## Intracellular Bactericidal Efficiency of BNPs and LPHNPs

J774.1 and RAW 264.7 cells ( $1.5 \times 10^5$  cells) were seeded in 24-well plates in DMEM with 10% FBS for 24 h. The cells were infected by *M. smegmatis* or *S. aureus* for 2h in DMEM at a multiplicity of infection (MOI) of 10 bacteria/cell. After 2 h, gentamicin (200  $\mu\text{g}/\text{mL}$ ) was added to kill the extracellular bacteria for 2h. After incubation, cells were washed with PBS, and free antibiotic(s) or antibiotic (doxycycline or vancomycin)-loaded BNPs or cationic, zwitterionic LPHNPs were added. After 24 h of incubation, the cells were washed with cold PBS three times, and the macrophages were treated with ice-cold sterilized MilliQ water to release the intracellular bacteria. The lysates were diluted, plated on agar plates, and cultured overnight at  $37^\circ\text{C}$ . Colony-forming units (CFU/mL) were calculated. The medium without the drug was used as a negative control.<sup>2,33</sup> The LIVE/DEAD BacLight Bacterial Viability Kit (Molecular Probes) was used to visualize the viable and dead bacterial cells within macrophages. As described above, the J774.1 or RAW 264.7 cells ( $1.5 \times 10^5$  cells) were seeded on a coverslip and the infection was established as described earlier in this section. Macrophages were incubated with a cocktail of the LIVE/DEAD BacLight bacterial viability staining solution for 15 min in the dark in the presence of TritonX. After washing with PBS, cells were visualized under confocal microscopy (TCS SP5 II; Leica).<sup>2</sup>

## Statistical Analysis

The Bonferroni posthoc test was used for comparisons between groups after at least three independent sets of experiments performed in triplicate. Differences were

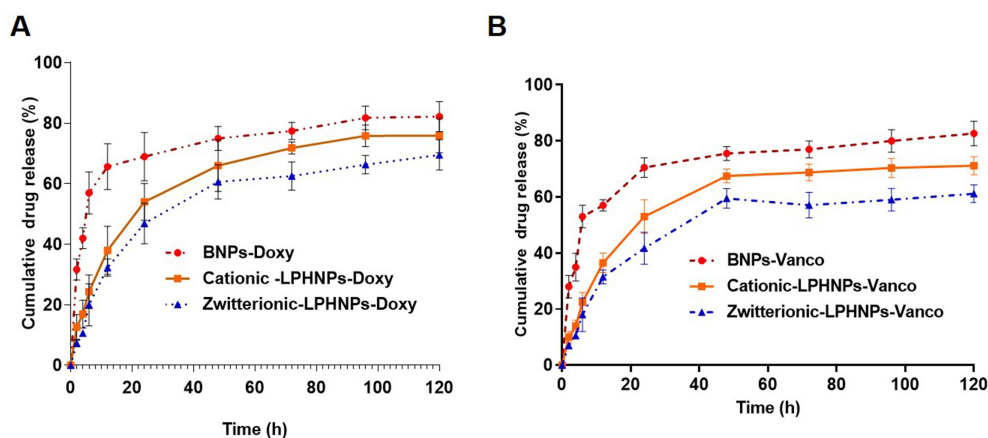


**Figure 3** In vitro antibiotic cumulative release from (A) doxycycline or (B) vancomycin loaded non-lipid layered BNPs and cationic or zwitterionic LPHNPs.

**Table 2** Details of Formulation and Characterization of Non-Lipid Layered BNPs and Cationic or Zwitterionic LPHNPs Loaded with Doxy or Vancomycin

Formulation -Group	Variations	Compositions	Z-Ave Size	PDI	Charge	EE%
Non-lipid layered NPs (F1)	NA	Bare PLGA NPs (without drug) (F1A)	226±9.6	0.191±0.023	-26±2.6	-
	NB	Bare PLGA NPs with doxycycline (F1B)	257±8.4	0.213±0.024	-27±3.7	63
	NC	Bare PLGA NPs with vancomycin (F1C)	249±5.4	0.19±0.023	-29±2.1	57
Cationic LPHNPs (F2)	CA	Cationic LPHNPs (without drug) (F2A)	203 ±6.6	0.178±0.017	+39±1.3	-
	CB	Cationic LPHNPs with doxycycline (F2B)	231±7.4	0.22±0.018	+38±3.4	71
	CC	Cationic LPHNPs with vancomycin (F2C)	223 ±6.2	0.2±0.02	+40±2.3	64
Zwitterionic LPHNPs (F3)	ZA	Zwitterionic LPHNP (without drug) (F3A)	191 ±5.4	0.147±0.017	-7±3.5	-
	ZB	Zwitterionic LPHNPs with doxycycline (F3B)	222 ±4.7	0.22±0.012	-8±2.8	79
	ZC	Zwitterionic LPHNPs With vancomycin (F3C)	214 ±3.3	0.19±0.017	-8±1.2	76

considered significant at  $P < 0.05$ . The Prism software package (version 5.02; GraphPad Software Inc., La Jolla, CA, USA) was used to perform the statistical tests.

#### Supporting Information

Description of details for demonstrating formulation, characterization, and Schematic outline of the preparation method for materials; additional confocal microscopy images, cell viability test, electron microscopy, DLS size distribution.

## Results

### Preparation and Characterization of Antibiotic-Loaded LPHNPs

We have previously demonstrated different methods of preparation and LPHNPs, and their characterization helped us to significantly improve the fabrication of the nanomaterials, control the size and the surface charge of LPHNPs, which further improved the reproducibility of our research.<sup>18,19,21</sup> Figure 1 and S1 describe the schematic diagram of the experimental design. Figure 2, S2, and Table 1 illustrate the production of different hybrid nanoformulations of drug-loaded cationic or zwitterionic LPHNPs and non-lipid layered bare nanoparticles (BNPs) using modified emulsion solvent-evaporation process and their physicochemical characteristics.<sup>19</sup> The size of hybrid nanoparticles (HNPs) is a critical parameter, with direct effects on cellular uptake, stability, and tissue

distribution.<sup>22–25</sup> Thus, we used dynamic light scattering (DLS) technology to determine the size range, size distribution (PDI), and zeta potential measurements to examine the surface charge of LPHNPs.<sup>16</sup> Based on DLS, the modified solvent evaporation method yielded relatively monodispersed LPHNPs and BNPs with a size range from 150–300 nm and narrow size distribution (PDI between 0.14–0.22). As summarized in Table 1 and illustrated in Figure 3A, the incorporation of cationic or zwitterionic lipids in the LPHNP formulation resulted in a significant reduction in size ( $P < 0.05$ ) compared to those of non-lipid layered formulations (BNPs). For instance, cationic (CA) or zwitterionic (ZA) LPHNPs were  $203 \pm 6.6$  and  $191 \pm 5.4$  nm, respectively, which were smaller than the non-lipid layered BNP formulation (NA), ie,  $226 \pm 9.6$  nm. Consistent with previous reports from our group and other research groups demonstrated that the incorporation of either cationic or zwitterionic lipids significantly reduce the size of formed NPs, which could be explained by the fact that the processing of those NPs in a single step was stabilized by the function of the lipids with an emulsifying agent, possibly reducing the coalescence of particles.<sup>15,19</sup>

We utilized a double emulsion solvent evaporation technique to enable the encapsulation of drugs (doxycycline or vancomycin), which drastically affected the size of these NPs, as indicated in Table 1. For instance, NA, CA,

and ZA were smaller than NB, NC, CB, CC, ZC. Additionally, BNP non-lipid layered formulations encapsulating doxycycline (NB) or vancomycin (NC) were larger than cationic and zwitterionic LPHNPs encapsulating doxycycline (CB and ZB) or vancomycin (CC and ZC). Surface charge is another critical factor that it dictates the NP interaction with cells, penetration, and plays an essential role in colloidal stability.<sup>12,24,26</sup> Thus, we investigated the surface charge (Zeta potential) of cationic (C) and zwitterionic (Z) LPHNPs and non-lipid layered BNPs (N) using the Zetasizer Nano ZS (Malvern Instruments, Malvern, UK).<sup>16,19</sup> As expected, the inclusion of either cationic or zwitterionic lipids with LPHNP formulations resulted in changes in the charged surface, as shown in Table 1 and Figure 2. Our results confirmed that the changes in surface charge of BNPs were not affected when an antibiotic was incorporated, ie, doxycycline (NB) or vancomycin (NCB). In contrast, the inclusion of either cationic (C) or zwitterionic (Z) lipids into the LPHNP formulation resulted in a charge reduction from  $-29 \pm 2.1$  mV towards positive or neutral values.<sup>18</sup>

As summarized in Table 1, the addition of cationic lipid to the NP formulations (CA, CB, and CC) resulted in positively charged surfaces, and the inclusion of a zwitterionic lipid to the NP formulations (ZA, ZB, and ZC) resulted in charge reductions from the native surface charge of BNPs ( $-29 \pm 2.1$  mV). The morphologies of antibiotic-encapsulated LPHNPs and BNPs were examined to ensure that they were hybrid nanoparticles with lipid and polymeric cores, rather than a random composition of liposomes and uncovered polymeric NPs.<sup>14,16,17</sup> As shown in Figure 2C and D; S1 (FESEM), the vancomycin or doxycycline-encapsulated BNPs and LPHNPs exhibited a nano-spherical shape, with no distinct morphological differences among the LPHNP groups. Additionally, EF-TEM images (Figure 2D) showed the core-shell hybrid structure of LPHNPs and confirmed the presence of the lipid layer on the PLGANP surfaces. Cryo-TEM microscopy was performed to inspect the LPHNP structures identified by FE-SEM and EF-TEM.<sup>27</sup> Both cationic and zwitterionic lipid layered LPHNPs exhibited a perfectly spherical shape (Figure 2), and the apparent particle sizes corresponded well to the NP sizes calculated by DLS (Table 1). Highly electron-dense structures on the LPHNPs, which were easily melted upon electron beam exposure, and extended and loose structures were present in the dispersed phase, as reported by Colombo et al.<sup>25</sup> To obtain direct evidence for lipid self-assembly on the PLGA

NP core, we incorporated fluorescent NBD-PC lipids into cationic or zwitterionic lipids. As shown in Figure 2, the CLSM image showed green fluorescence indicating a perfect nanosphere shell layer, demonstrating that the efficient and straightforward process led to the formation of lipid layered hybrid nanoparticles.<sup>28</sup> The stability of antibiotic-encapsulated LPHNPs and BNPs was examined to ensure that the formulations are appropriate for prolonged storage and commercial feasibility. The z-average size was used to study NP stability by DLS at specific intervals. As shown in Figure S6 all the LPHNP formulations stored at 4°C remained stable during the entire observation period of two weeks. However, the z-average was slightly higher than the size when it was produced on the first day and showing no visible signs of instability, such as no sedimentation or aggregation.

The drug entrapment efficiencies for vancomycin- or doxycycline-encapsulated BNPs and LPHNPs were shown in Figure 1 summarized in Table 1. The DLS results showed that antibiotic encapsulation in LPHNPs and BNPs resulted in a moderate size increase. The encapsulation efficiencies of doxycycline -BNPs (NB) and cationic or zwitterionic lipid-layered LPHNPs (CB, and ZB) were 63%, 71%, and 79%, respectively. We also observed that the vancomycin encapsulation efficiencies of BNPs (NC) and cationic or zwitterionic lipid layered LPHNPs (CC and ZC) were 57%, 64%, and 76%, respectively. The drug incorporation efficiency of hydrophilic antibiotics in non-lipid layered formulations (BNPs) was lower than that in lipid layered formulations.

## In vitro Drug Release from LPHNPs and BNPs

The cumulative antibiotic release from doxycycline- or vancomycin-encapsulated BNPs and cationic or zwitterionic lipid-layered LPHNPs were assessed for 120 h. As shown in Figure 3, the cationic (C) or zwitterionic (Z) lipid layered LPHNPs displayed the controlled release of doxycycline or vancomycin with minimal burst release. In contrast, non-lipid layered BNPs (N) showed an initial burst release, followed by sustained drug release.<sup>29,30</sup> For instance, the antibiotic release rates of doxycycline-BNPs (NB) at 12, 24, and 48 h were 65%, 69%, and 75%, respectively, while doxycycline release rates from cationic (CB) and zwitterionic (ZB) lipid-layered LPHNPs at 24, 48, and 72 h were 38%, 54%, and 66% and 32%, 47%, and 61%, respectively. Similarly, the cationic (CB) and zwitterionic (ZB)

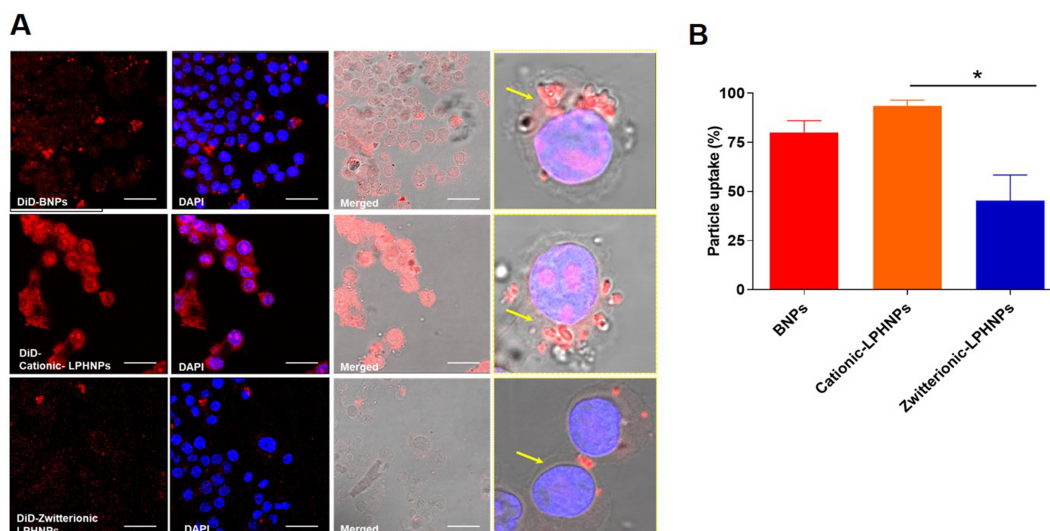


**Figure 4** Effect of surface characteristics of NPs on macrophage cellular uptake and intracellular behaviors. Fluorescent NPs (DiD labeled BBNPs and cationic and zwitterionic LPHNPs) were treated with J774.1 cell (labeled with DAPI) for 24 hours, and then the particle uptake efficiency was visualized by (A) Confocal microscopy images (Scale bar 50um) and quantified by (B) flow cytometry. (Yellow arrow- The presence of particles inside the macrophage. \* $p < 0.05$ ; Statistically significant).

International Journal of Nanomedicine downloaded from https://www.dovepress.com/ by 165.194.103.27 on 31-Dec-2020  
For personal use only.

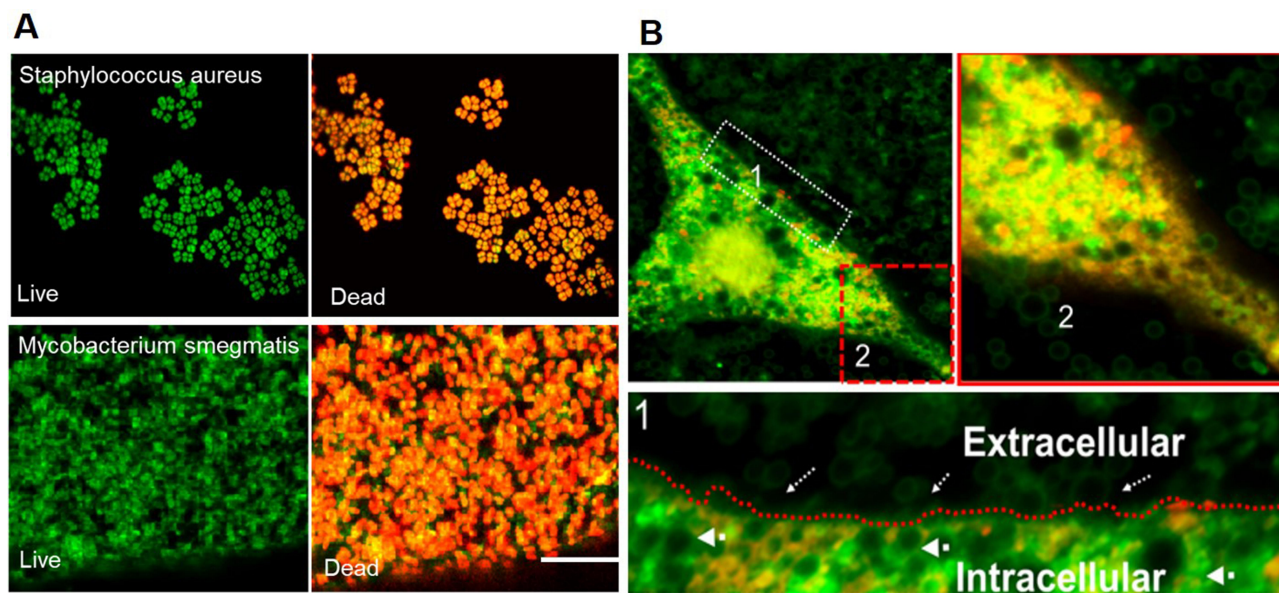


**Figure 5** (A) Representative CLSM images of the viable and dead intracellular *S.aureus* and *M.smegmatitis*. Figure (B) shows the adhesion of cationic LPHNPs -doxy on the surface of macrophages (dotted white arrow indicating LPHNPs on the extracellular leaflet and a thick arrow indicating LPHNPs in the intracellular compartment of macrophages. Inlet Figure (B) shows the live (green) and dead bacteria (red) (post-treatment) with LPHNPs.

lipid-layered LPHNPs encapsulated Vanco had a slower release rate than the non-lipid layered BNP-vancomycin formulation (ZC). As shown in Figure 3, the amount of vancomycin released from BBNPs were 57%, 70%, and 76% at 12, 24, and 48 h, respectively. In comparison, the amount of vancomycin released from cationic (CC) and zwitterionic (ZC) lipid layered LPHNPs at the same time values were 37%, 53%, and 68% and 32%, 42%, and 60%, respectively.

Furthermore, all LPHNP formulations exhibited minimal burst release with the controlled antibiotic release, unlike the non-lipid layered BBNPs, which exhibit higher initial burst release followed by controlled drug release kinetics. The lipid layer could likely explain this difference on the NP core, which could slow the drug release kinetics by acting as a molecular fence between the polymeric matrix and aqueous phase.<sup>17,18</sup>



## Antibacterial Activity Against *Staphylococcus aureus* or *Mycobacterium smegmatis*

*S. aureus* and *M. smegmatis* were used to investigate the bactericidal activity of free antibiotics and doxycycline- or vancomycin-encapsulated cationic (C) or zwitterionic (Z) lipid-layered LPHNPs and BNPs (F1) by broth-microdilution assay. Antibiotic-loaded cationic (C) or zwitterionic (Z) LPHNP and BNP (N) formulations were directly incubated with a suspension of *M. smegmatis* or *S. aureus* at 37°C.<sup>2</sup> The MIC values for all of the doxycycline- or vancomycin-loaded cationic (C) or zwitterionic (Z) LPHNP and BNP (N) formulations are presented in Table 2. All the tested doxycycline- or vancomycin-loaded cationic (F2) or zwitterionic (F3) LPHNP and BNP (F1) formulations inhibited the growth of *M. smegmatis* or *S. aureus*, as presented in Table 2. The MIC of free Doxy was 4 µg/mL; however, cationic LPHNP-Doxy (F2B) showed a MIC of 4 µg/mL against *M. smegmatis*, indicating that the formulations exhibited the same MIC as the free antibiotic. Besides, our results demonstrated that the synergism between the antibiotics and cationic-LPHNPs enhanced the antibacterial activity against *S. aureus* and *M. smegmatis*. Our plausible explanation for the enhanced in vitro antibacterial activity is the combinatorial antibacterial effect of the antibiotic and physicochemical properties, such as the size and charge of the lipid layer LPHNPs.<sup>31</sup> We demonstrated that the cationic charge of DOTAP promoted stronger adhesion to the negatively charged bacteria, such as *S. aureus* and *M. smegmatis* ( $-42.9 \pm 5.9$  mV).<sup>31,32</sup> Additionally, our experimental observations strongly suggested a synergistic antibacterial effect of the cationic surface of LPHNPs (C) and encapsulated antibiotics (doxycycline or vancomycin). However, synergistic effects were not observed for the zwitterionic or anionic surfaces of LPHNPs (Z) or BNPs (N) and encapsulated antibiotics.

### Cytotoxicity

Cationic lipids exhibit moderate to high cytotoxicity. Our experimental results confirmed similar cytotoxicity for cationic LPHNPs and BNP- doxycycline or vancomycin formulations, as shown in Figure S5. Notably, at a low NP concentration (10 µg/mL), all LPHNPs and BNPs exhibited low cytotoxicity (cell viability >80%). However, when the NP concentration increased, cell viability decreased. Zwitterionic LPHNPs did not affect cell viability, even at

a higher NP concentration (60 µg), which can likely be explained by the biomimetic effect of PC lipids.

### Surface Charge of LPHNPs Influence the Macrophages Uptake

After red fluorescent dye (DiD) was encapsulated within LPHNPs and BNPs, particle uptake (LPHNPs and BNPs) by J774.1 cells were quantified by flow cytometry and further visualized by confocal microscopy.<sup>2,19</sup> After 24 h of incubation, the BNPs and cationic-LPHNPs were more efficiently taken up by J774.1 cell than the zwitterionic LPHNPs (Figure 4). The intracellular distribution of fluorescently labeled NPs was further analyzed by CLSM to confirm that NPs were present in the cells rather than absorbed into the cell membrane.<sup>33</sup> Figure 5 shows that the cationic LPHNPs (C) surfaces were more rapidly recognized and processed by phagocytes than the zwitterionic surfaces (Z). Furthermore, cationic LPHNPs (C) show higher uptake, nearly 93%, followed by BNPs, were 80%, respectively. Interestingly, zwitterionic LPHNPs were taken by macrophages less efficiently (49%) as compared to cationic and non-lipid layered NPs. These results depict that macrophage recognition, uptake efficiency, and subsequent intracellular trafficking of tested nanocarriers is positively correlated with the surface properties.

### Intracellular Antibacterial Activity of LPHNPs and BNP

The intracellular antimicrobial activity of cationic or zwitterionic LPHNPs and non-lipid layered BNPs were tested in macrophages in vitro. Free doxycycline or vancomycin treatment decreased the intracellular bacterial load (2-log-CFU compared with the initial infection) for *M. smegmatis* and *S. aureus* (Figure 5). Treatment with cationic LPHNP-doxycycline (CB) and LPHNP-vancomycin (CC) resulted in a reduction of 4 or 3 log CFU compared with the untreated infected cells, as shown in (Figures 6 and 7). Similarly, treatment with non-lipid layered BNPs encapsulating doxycycline (NB), and vancomycin (NC) resulted in bacterial reductions of 3 and 2 log CFU compared with the initial infection. However, zwitterionic LPHNP-doxycycline (CB) and LPHNP-vancomycin (CC) showed moderate reductions of intracellular antibacterial activity (2 and 1 log CFU) as compared to the initial infection. To confirm the intracellular antibacterial activity, confocal microscopy was performed using LIVE/DEAD BacLight bacterial viability assays to

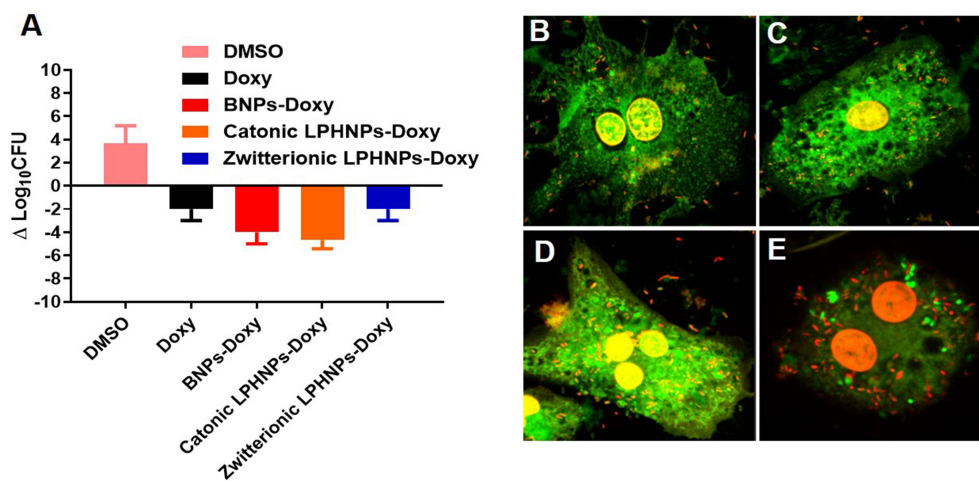


**Figure 6** Intracellular bactericidal (*M. smegmatis*) activity of doxycycline loaded non-lipid layered BNPs and cationic or zwitterionic LPHNPs. **(A)** Intracellular killing efficiency of doxycycline loaded non-lipid layered BNPs and cationic or zwitterionic LPHNPs was investigated with controls (free drug and DMSO). **(B–E)** Representative CLSM images of the viable and dead intracellular mycobacterium within macrophages after the treatment with the free drug, doxycycline loaded non-lipid layered BNPs and cationic or zwitterionic LPHNPs.

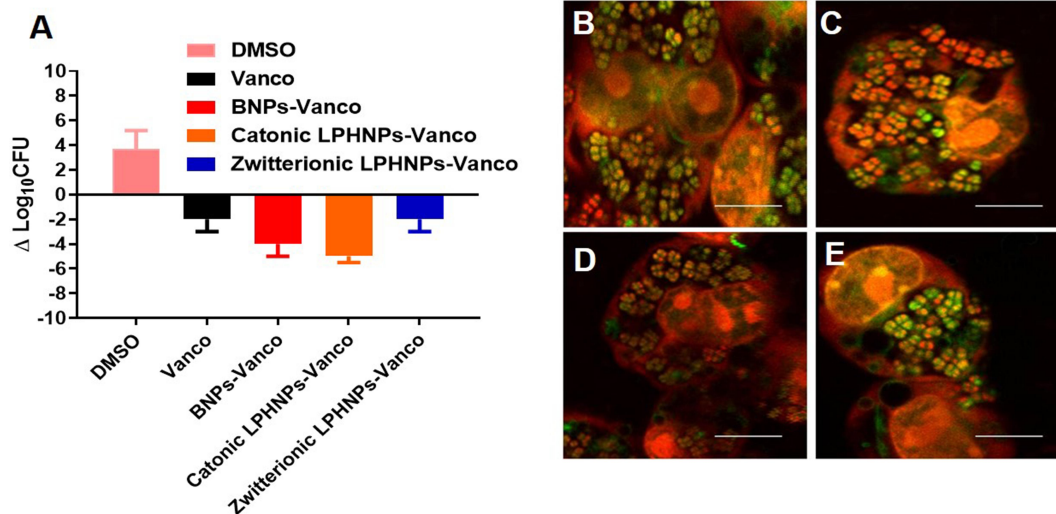


**Figure 7** Intracellular bactericidal (*S. aureus*) activity of vancomycin loaded non-lipid layered BNPs and cationic or zwitterionic LPHNPs. **(A)** Intracellular killing efficiency of vancomycin loaded non-lipid layered BNPs, and cationic or zwitterionic LPHNPs was investigated with controls (free drug and DMSO). **(B–E)** Representative confocal microscopy images of the viable and dead intracellular *S. aureus* within macrophages after the treatment with the free drug, doxycycline loaded non-lipid layered BNPs and cationic or zwitterionic LPHNPs.

distinguish between dead (labeled in red) and live bacteria (labeled in green) within macrophages<sup>2</sup> after treatment (Figures S3 and S4). Figure 5 illustrates the intracellular antibacterial activity obtained after different NPs formulations and free antibiotics. Intracellular *M. smegmatis* and *S. aureus* were alive in macrophages after treatment with a free antibiotic (doxycycline or vancomycin), which demonstrated that the limited entry of free antibiotics inside the macrophages. On the contrary, the treatment with either cationic LPHNPs loaded with doxycycline or

vancomycin resulted in a bacterial CFU reduction compared to the free drug in bacterial counts, which represented a reduction of 80% intracellular bacteria replication compared to the untreated infected cells. Treatment with BNP-antibiotic (doxycycline or vancomycin) effectively killed most intracellular *M. smegmatis* or *S. aureus* and treatment with zwitterionic LPHNP-antibiotic formulations were moderately effective in the eradication of intracellular pathogens. These results indicated that the surface charge of nanocarriers plays

a crucial role in NP uptake, thereby influencing the intracellular antibacterial efficacy.

## Discussion

Developing correlations between nanoparticle physicochemical characteristics and their uptake and intracellular trafficking mechanisms in macrophages would provide a basis to overcome the intracellular antibiotic delivery and targeting, and facilitate the design of new, more effective, and safer nanomaterial platforms.<sup>12,34</sup> However, intracellular infections remain a challenging task for physicians to eradicate, mainly due to the poor intracellular penetration of most of the commonly used antibiotics. Bacteria use macrophages as a “Trojan horse” to induce a secondary site of infection, thereby causing persistent or recurrent infections.<sup>12</sup> Therefore, we performed a representative study to investigate the effect of cationic or zwitterionic LPHNPs, when compare to non-lipid layered BNPs. The encapsulation of doxycycline or vancomycin within the polymeric matrix protected the drug from degradation. Doxycycline is a broad-spectrum tetracycline-based antibiotic, which exerts bactericidal action by inhibiting protein synthesis.<sup>30,35</sup> Vancomycin is the most commonly used antibiotic for *S. aureus* infections; it inhibits the biosynthesis of peptidoglycan and the assembly of NAM–NAG–polypeptide in the peptidoglycan chain.<sup>5,29</sup> Overall, our experimental data indicated that the encapsulation of doxycycline or vancomycin into the LPHNPs or BNPs significantly reduced the antibacterial efficacy, but may have prolonged activity by extending the time of action of a single dose as compared to that for free antibiotics.<sup>5,30,35,36</sup> This improved antibiotic entrapment ability of LPHNPs can be explained by the ability of lipids to act as a molecular fence, which prevents drug leakage in the external phase during the solvent evaporation process, consistent with the results of Zhang et al (2008).<sup>17</sup> The cationic surface nature of LPHNPs promoted the higher macrophage recognition and uptake of NPs and thereby enhances the intracellular bacterial killing efficiency. These results are critical for building the knowledge base required to design efficient and specific LPHNP-based nano-antibiotics and nanoparticles based hand sanitizers.<sup>37,38</sup>

## Conclusion

In summary, a comprehensive proof of concept investigation demonstrates that the effects on changes in surface charge result in enhanced macrophage uptake. Out of anionic, cationic, and zwitterionic charged formulations, cationic loaded LPHNPs demonstrated the enhanced

intracellular bacterial killing efficiency that was loaded with either doxycycline or vancomycin cleared the phagocytosed *M. smegmatis*- or *S. aureus* bacteria in macrophages, providing a basis for optimizing their use in biomedical applications.

## Acknowledgments

This research was supported by Creative Materials Discovery Program through the National Research Foundation of Korea (NRF) funded by the Ministry of Science and ICT (NRF-2018M3D1A1058813), This research was supported by the National Research Foundation of Korea (NRF) funded by the Ministry of Science and ICT (NRF-2019R1A2C1007088), and Dongguk University Research Fund of 2018.

## Author Contributions

All authors contributed to data analysis, drafting or revising the article, have agreed on the journal to which the article was submitted, gave final approval of the version to be published, and agree to be accountable for all aspects of the work.

## Disclosure

The authors report no conflicts of interest for this work.

## References

1. Armstead AL, Li B. Nanomedicine as an emerging approach against intracellular pathogens. *Int J Nanomedicine*. 2011;6(1):3281–3293.
2. Abed N, Said-Hassane F, Zouhiri F, et al. An efficient system for intracellular delivery of beta-lactam antibiotics to overcome bacterial resistance. *Sci Rep*. 2015;5(1). doi:10.1038/srep13500.
3. Imbuluzqueta E, Gamazo C, Ariza J, Blanco-Prieto MJ. *Drug Delivery Systems for Potential Treatment of Intracellular Bacterial Infections*. 2010.
4. Pelgrift RY, Friedman AJ. Nanotechnology as a therapeutic tool to combat microbial resistance. *Adv Drug Deliv Rev*. 2013;65(13):1803–1815. doi:10.1016/j.addr.2013.07.011
5. Seedat N, Kalhapure RS, Mocktar C, et al. Co-encapsulation of multi-lipids and polymers enhances the performance of vancomycin in lipid-polymer hybrid nanoparticles: in vitro and in silico studies. *Mater Sci Eng C*. 2016;61:616–630. doi:10.1016/j.msec.2015.12.053
6. Gao W, Thamphiwatana S, Angsantikul P, Zhang L. Nanoparticle approaches against bacterial infections. *Wiley Interdiscip Rev Nanomed Nanobiotechnol*. 2014;6(6):532–547.
7. Seo Y, Kim J-E, Jeong Y, et al. Engineered nanoconstructs for the multiplexed and sensitive detection of high-risk pathogens. *Nanoscale*. 2016;8(4):1944–1951. doi:10.1039/C5NR06230F
8. Zhu Y, Ramasamy M, Yi DK. Antibacterial activity of ordered gold nanorod arrays. *ACS Appl Mater Interfaces*. 2014;6(17):15078–15085. doi:10.1021/am503153v
9. Jeong H, Heo J, Son B, et al. Intrinsic hydrophobic cairnlike multi-layer films for antibacterial effect with enhanced durability. *ACS Appl Mater Interfaces*. 2015;7(47):26117–26123. doi:10.1021/acsami.5b07613

10. Hwangbo S, Jeong H, Heo J, et al. Antibacterial nanofilm coatings based on organosilicate and nanoparticles. *React Funct Polym*. 2016;102:27–32. doi:10.1016/j.reactfunctpolym.2016.03.004
11. Pinto-Alphandary H, Andrement A, Couvreur P. Targeted delivery of antibiotics using liposomes and nanoparticles: research and applications. *Int J Antimicrob Agents*. 2000;13(3):155–168. doi:10.1016/S0924-8579(99)00121-1
12. Bose RJ, Tharmalingam N, Garcia Marques FJ, et al. Reconstructed apoptotic bodies as targeted “nano decoys” to treat intracellular bacterial infections within macrophages and cancer cells. *ACS Nano*. 2020;14(5):5818–5835. doi:10.1021/acsnano.0c00921
13. Huh AJ, Kwon YJ. “Nanoantibiotics”: a new paradigm for treating infectious diseases using nanomaterials in the antibiotics resistant era. *J Control Release*. 2011;156(2):128–145. doi:10.1016/j.jconrel.2011.07.002
14. Mandal B, Bhattacharjee H, Mittal N, et al. Core–shell-type lipid–polymer hybrid nanoparticles as a drug delivery platform. *Nanomedicine*. 2013;9(4):474–491. doi:10.1016/j.nano.2012.11.010
15. Rajendran JC, Bose J-CA, Yoshie A, Parka S, Park H, Lee S-H. Soo-Hong Lee preparation of cationic lipid layered PLGA hybrid nanoparticles for gene delivery. *J Control Release*. 2015;213:e92–e93. doi:10.1016/j.jconrel.2015.05.154
16. Rajendran JC, Bose S-HL, Park H. Biofunctionalized nanoparticles: an emerging drug delivery platform for various disease treatments. *Drug Discov Today*. 2016.
17. Zhang L, Chan JM, Gu FX, et al. Self-assembled lipid–polymer hybrid nanoparticles: a robust drug delivery platform. *ACS Nano*. 2008;2(8):1696–1702. doi:10.1021/nm800275r
18. Bose RJ, Lee S-H, Park H. Lipid polymer hybrid nanospheres encapsulating antiproliferative agents for stent applications. *J Ind Eng Chem*. 2016;36:284–292. doi:10.1016/j.jiec.2016.02.015
19. Bose RJC AY, Ahn JC, Park H, Lee SH. Influence of cationic lipid concentration on properties of lipid–polymer hybrid nanospheres for gene delivery. *Int J Nanomedicine*. 2015;2015(10):5367–5382.
20. Rajendran JCB, Byoung-Ju K, Lee SH, Park H. Surface modification of polymeric nanoparticles with human adipose derived stem cell membranes AdMSCs. *Front Bioeng Biotechnol*. 2016.
21. Bose RJC, Ravikumar R, Karuppagounder V, Bennet D, Rangasamy S, Thandavarayan RA. Lipid-polymer hybrid nanoparticle-mediated therapeutics delivery: advances and challenges. *Drug Discov Today*. 2017;22(8):1258–1265. doi:10.1016/j.drudis.2017.05.015
22. Hu C-MJ, Fang RH, Wang K-C, et al. Nanoparticle biointerfacing by platelet membrane cloaking. *Nature*. 2015;526(7571):118–121. doi:10.1038/nature15373
23. Benne N, van Duijn J, Kuiper J, Jiskoot W, Slütter B. Orchestrating immune responses: how size, shape and rigidity affect the immunogenicity of particulate vaccines. *J Control Release*. 2016;234:124–134. doi:10.1016/j.jconrel.2016.05.033
24. Jiang Y, Huo S, Mizuhara T, et al. The interplay of size and surface functionality on the cellular uptake of sub-10 nm gold nanoparticles. *ACS Nano*. 2015;9(10):9986–9993. doi:10.1021/acsnano.5b03521
25. Krishnakumar D, Kalaiyarasi D, Bose J, Jaganathan K. Evaluation of mucoadhesive nanoparticle based nasal vaccine. *J Pharm Investig*. 2012;42(6):315–326. doi:10.1007/s40005-012-0042-3
26. Yu SS, Lau CM, Thomas SN, et al. Size-and charge-dependent non-specific uptake of PEGylated nanoparticles by macrophages. *Int J Nanomedicine*. 2012;7:799–813. doi:10.2147/IJN.S28531
27. Colombo S, Cun D, Remaut K, et al. Mechanistic profiling of the siRNA delivery dynamics of lipid–polymer hybrid nanoparticles. *J Control Release*. 2015;201:22–31. doi:10.1016/j.jconrel.2014.12.026
28. Shi J, Xiao Z, Votruba AR, Vilos C, Farokhzad OC. Differentially charged hollow core/shell lipid–polymer–lipid hybrid nanoparticles for small interfering RNA delivery. *Angew Chem*. 2011;123(31):7165–7169. doi:10.1002/ange.201101554
29. Zakeri-Milani P, Loveymi BD, Jelvehgari M, Valizadeh H. The characteristics and improved intestinal permeability of vancomycin PLGA-nanoparticles as colloidal drug delivery system. *Colloids Surf B Biointerfaces*. 2013;103:174–181. doi:10.1016/j.colsurfb.2012.10.021
30. Misra R, Acharya S, Dilnawaz F, Sahoo SK. Sustained antibacterial activity of doxycycline-loaded poly (D, L-lactide-co-glycolide) and poly ( $\epsilon$ -caprolactone) nanoparticles. *Nanomedicine*. 2009;4(5):519–530. doi:10.2217/nmm.09.28
31. Chenevier P, Veyret B, Roux D, Henry-Toulme N. Interaction of cationic colloids at the surface of J774 cells: a kinetic analysis. *Biophys J*. 2000;79(3):1298–1309. doi:10.1016/S0006-3495(00)76383-1
32. Ayala-Torres C, Hernández N, Galeano A, Novoa-Aponte L, Soto C-Y. Zeta potential as a measure of the surface charge of mycobacterial cells. *Ann Microbiol*. 2014;64(3):1189–1195. doi:10.1007/s13213-013-0758-y
33. Mu H, Tang J, Liu Q, Sun C, Wang T, Duan J. Potent antibacterial nanoparticles against biofilm and intracellular bacteria. *Sci Rep*. 2016;6.
34. Li Y, Liu Y, Ren Y, et al. Coating of a novel antimicrobial nanoparticle with a macrophage membrane for the selective entry into infected macrophages and killing of intracellular staphylococci. *Adv Funct Mater*. 2020:2004942.
35. Franklin RK, Marcus SA, Talaat AM, et al. A novel loading method for doxycycline liposomes for intracellular drug delivery: characterization of in vitro and in vivo release kinetics and efficacy in a J774A. 1 cell line model of mycobacterium smegmatis infection. *Drug Metab Dispos*. 2015;43(8):1236–1245. doi:10.1124/dmd.115.063602
36. Sande L, Sanchez M, Montes J, et al. Liposomal encapsulation of vancomycin improves killing of methicillin-resistant *Staphylococcus aureus* in a murine infection model. *J Antimicrob Chemother*. 2012;67(9):2191–2194. doi:10.1093/jac/dks212
37. Jing JLL, Yi T P, Bose RJ, McCarthy JR, Tharmalingam N, Madheswaran T. Hand sanitizers: a review on formulation aspects, adverse effects, and regulations. *Int J Environ Res Public Health*. 2020;17(9):3326. doi:10.3390/ijerph17093326
38. Nakamura S, Sato M, Sato Y, et al. Synthesis and application of silver nanoparticles (Ag NPs) for the prevention of infection in healthcare workers. *Int J Mol Sci*. 2019;20(15):3620. doi:10.3390/ijms20153620
39. Ramasamy M, Lee SS, Yi DK, Kim K. Magnetic, optical gold nanorods for recyclable photothermal ablation of bacteria. *J Mater Chem B*. 2014;2(8):981–988. doi:10.1039/c3tb21310b
40. Bershteyn A, Chaparro J, Yau R, et al. Polymer-supported lipid shells, onions, and flowers. *Soft Matter*. 2008;4(9):1787–1791.
41. Yücel Ç, Değim Z, Yılmaz Ş. Nanoparticle and liposome formulations of doxycycline: transport properties through Caco-2 cell line and effects on matrix metalloproteinase secretion. *Biomed Pharmacother*. 2013;67(6):459–467. doi:10.1016/j.biopha.2013.03.001
42. Chakraborty SP, Sahu SK, Pramanik P, Roy S. In vitro antimicrobial activity of nanoconjugated vancomycin against drug resistant *Staphylococcus aureus*. *Int J Pharm*. 2012;436(1):659–676. doi:10.1016/j.ijpharm.2012.07.033
43. Jayamani E, Tharmalingam N, Rajamuthiah R, et al. Characterization of a francisella tularensis-caenorhabditis elegans pathosystem for the evaluation of therapeutic compounds. *Antimicrob Agents Chemother*. 2017;61(9):e00310–00317.
44. Tharmalingam N, Port J, Castillo D, Mylonakis E. Repurposing the anthelmintic drug niclosamide to combat helicobacter pylori. *Sci Rep*. 2018;8(1):3701. doi:10.1038/s41598-018-22037-x

## International Journal of Nanomedicine

Dovepress

### Publish your work in this journal

The International Journal of Nanomedicine is an international, peer-reviewed journal focusing on the application of nanotechnology in diagnostics, therapeutics, and drug delivery systems throughout the biomedical field. This journal is indexed on PubMed Central, MedLine, CAS, SciSearch<sup>®</sup>, Current Contents<sup>®</sup>/Clinical Medicine,

Journal Citation Reports/Science Edition, EMBase, Scopus and the Elsevier Bibliographic databases. The manuscript management system is completely online and includes a very quick and fair peer-review system, which is all easy to use. Visit <http://www.dovepress.com/testimonials.php> to read real quotes from published authors.

Submit your manuscript here: <https://www.dovepress.com/international-journal-of-nanomedicine-journal>